

# Induction of metastatic cancer stem cells from the NK/LAK-resistant floating, but not adherent, subset of the UP-LN1 carcinoma cell line by IFN- $\gamma$

Hung-Chang Chen<sup>1,\*</sup>, Andy Shau-Bin Chou<sup>2,\*</sup>, Yu-Chen Liu<sup>2</sup>, Chin-Hsuan Hsieh<sup>1</sup>, Chen-Chen Kang<sup>2</sup>, See-Tong Pang<sup>3</sup>, Chi-Tai Yeh<sup>4,5,6</sup>, Hui-Ping Liu<sup>3</sup> and Shuen-Kuei Liao<sup>1,2,6,7</sup>

As an advanced status of cancer stem cells (CSCs), metastatic CSCs (mCSCs) have been proposed to be the essential seeds that initiate tumor metastasis. However, the biology of mCSCs is poorly understood. In this study, we used a lymph node (LN) metastatic CEA-producing carcinoma cell line, UP-LN1, characterized by the persistent appearance of adherent (A) and floating (F) cells in culture, to determine the distribution of CSCs and mechanisms for the induction of mCSCs. F and A cells displayed distinct phenotypes, CD44<sup>high</sup>/CD24<sup>low</sup> and CD44<sup>low</sup>/CD24<sup>high</sup>, respectively. The CSC-rich nature of F cells was typified by stronger expression of multiple drug resistance genes and a 7.8-fold higher frequency of tumor-initiating cells in NOD/SCID mice when compared with A cells. F cells showed a greater depression in HLA class I expression and an extreme resistance to NK/LAK-mediated cytotoxicity. Moreover, the NK/LAK-resistant F cells were highly susceptible to IFN- $\gamma$ -mediated induction of surface CXCR4, with concomitant downregulation of cytoplasmic CXCL12 expression, whereas these two parameters remained essentially unchanged in NK/LAK-sensitive A cells. Following the induction of surface CXCR4, enhanced migratory/invasive potential of F cells was demonstrated by *in vitro* assays. Confocal immunofluorescence microscopy showed the two distinct phenotypes of F and A cells could be correspondingly identified in monodispersed and compact tumor cell areas within the patient's LN tumor lesion. In response to IFN- $\gamma$  or activated NK/LAK cells, the CXCR4<sup>+</sup> mCSCs could be only induced from the CSCs, which were harbored in the highly tumorigenic CD44<sup>high</sup>/CD24<sup>low</sup> F subset. Our results revealed the complexity and heterogeneity of the CSC of this cell line/tumor and the differential immunomodulatory roles of F and A cells. A better understanding of the interactions among different classes of CSCs and their niches may assist us in eradicating the CSCs/mCSCs through targeted immunotherapy, chemotherapy, or both.

*Laboratory Investigation* (2011) 91, 1502–1513; 10.1038/labinvest.2011.91; published online 20 June 2011

**KEYWORDS:** CD44/CD24; CXCR4/CXCL12 axis; HLA class I; metastasis; metastatic cancer stem cells; non-MHC-restricted effector lymphocytes

Metastasis is the major cause of death in patients with various cancers. The recently proposed cancer stem cell (CSC) hypothesis provides a new direction for the understanding of tumor metastasis.<sup>1</sup> To date, the possible existence of CSCs has been reported first in leukemia<sup>2</sup> and then in solid tumors including brain tumor,<sup>3,4</sup> breast cancer,<sup>5</sup> pancreatic cancer,<sup>6</sup> nasopharyngeal carcinoma,<sup>7</sup> and cancer of gastrointestinal tract<sup>8</sup> by using various CSC markers and approaches. In

contrast to the traditional stochastic model assuming that every single cell within the heterogeneous tumor has the ability to generate a tumor, the CSC hypothesis emphasizes the stem cell hierarchy constructed by the heterogeneous tumor cells, in which there is only a rare specific population of tumor-initiating cells (TICs) with the stem cell properties, including self-renewal and the ability to give rise to the majority of differentiated cell populations.<sup>9,10</sup> The stem-like

<sup>1</sup>Graduate Institute of Biomedical Sciences, Chang Gung University, Taoyuan, Taiwan; <sup>2</sup>Graduate Institute of Clinical Medical Sciences, Chang Gung University, Taoyuan, Taiwan; <sup>3</sup>Department of Surgery, Chang Gung Memorial Hospital, Taoyuan, Taiwan; <sup>4</sup>Graduate Institute of Clinical Medicine, Taipei Medical University, Taipei, Taiwan; <sup>5</sup>Cancer Center, Shuan Ho Hospital, Taipei Medical University, Taipei, Taiwan; <sup>6</sup>Center of Excellence for Cancer Research, Taipei Medical University, Taipei, Taiwan and <sup>7</sup>Cancer Immunotherapy Center and Department of Radiation Oncology, Cancer Center, Taipei Medical University Hospital, Taipei, Taiwan  
Correspondence: Dr S-K Liao, PhD, Cancer Immunotherapy Center and Department of Radiation Oncology, Cancer Center, Taipei Medical University Hospital, 252 Wu-Hsing Street, Taipei 110, Taiwan.  
E-mail: liaosk@tmuh.org.tw

\*These authors equally contributed to this work.

Received 26 December 2010; revised 17 April 2011; accepted 18 April 2011

properties of the TICs provide great plasticity for these tumor cells to adapt and colonize in the new metastatic site, orchestrated by normal stromal cells, bone marrow-derived mesenchymal stem cells,<sup>11</sup> and immune cells including myelomonocytic cells.<sup>12</sup> All of these cell components and the tissue matrix constitute a 'tumor microenvironment', and are important factors for tumor progression. Moreover, the CSC concept has been proposed to further contribute to resistances to drugs<sup>13</sup> and radiation<sup>14</sup>, recurrences after chemo- and immunotherapy,<sup>15</sup> and tumor dormancy.<sup>16</sup>

As only a limited cell lines have been established from lymph node (LN) or other metastatic sites and are currently available for the study of CSCs in metastases,<sup>17–19</sup> we have recently established a CEA-producing carcinoma cell line, UP-LN1, from a patient with unknown primary, and documented some of its immunophenotypic and molecular cytogenetic features.<sup>20</sup> The demonstrated phenotype, CK7<sup>-</sup>/CK20<sup>+</sup>/CEA<sup>+</sup>/SCCA<sup>-</sup>, made the gastrointestinal tract the most probable primary site. Consistent with the coexistence of singly dispersed or small clumps of cells and tightly compact solid tumor cells observed within the LN biopsy structure in which was largely replaced by tumor cells, the persistent appearance of naturally occurring adherent (A) and floating (F) cells was noted in culture. Such an *in vitro* mixed phenotype has not frequently been reported in cultures of human carcinomas of diverse histological types.<sup>21</sup> The existence of such cells has, thus, often been ignored, and consequently these floating cells have been discarded during cell passages of various cancer cell lines by many investigators.<sup>21,22</sup> Therefore, the nature of such adherent cells *vs* floating cells remains largely uninvestigated.

We hypothesized that A and F cells of the UP-LN1 cell line might differently harbor CSCs, and could thus differently contribute to the metastatic potential of tumor in the patient. In this study, we enriched A and F cell subsets and determined the differences between these two cell types with respect to cancer stem-like cell properties, relative drug resistance, immunophenotype, anchorage-independent clonogenicity, sensitivity to NK/LAK cytotoxicity, migration/invasion ability, and tumorigenicity in NOD/SCID mice. We found that as the major niche for metastatic CSCs (mCSCs), the CD44<sup>high</sup>/CD24<sup>low</sup> F cells, but not CD44<sup>low</sup>/CD24<sup>high</sup> A cells, expressed lower levels of surface HLA class I and at the same time harbored a specific subset of NK/LAK-resistant CSCs, which turned out to be highly susceptible to IFN- $\gamma$ -mediated induction of CXCR4<sup>+</sup> mCSCs.

## MATERIALS AND METHODS

### Cell Lines and Culture Conditions

The UP-LN1 cell line and its A and F subsets, K562, and Daudi cell lines were used in this study. Unless specified, all the cell lines were maintained in the condition described previously.<sup>20</sup> For the separation of A cells, we discarded all floating cells in the culture supernatant and then harvested only the adherent cells by light trypsinization to set up new

cultures for A cells. To obtain F cells, we only collected the floating cells in the culture supernatant of UP-LN1 culture for the subsequent culture passage. Each of these two protocols was used for the enrichment of A or F cells when subculturing for 10 consecutive rounds. To maintain the parental UP-LN1 (P) cells, floating cells and trypsinized adherent cells were washed and pooled, followed by setting up a new culture in our routine cell line maintenance. Trypan blue dye exclusion was used to monitor the cell viability.

A and F cells were also compared for their growth in RPMI-1640 medium supplemented with 10% FBS (RPMI medium) and in HEScGRO medium (Chemicon, Temecula, CA, USA) independently; the latter has been used to support the growth of human embryonic stem cells.

### Cytofluorometric Analysis

Indirect immunofluorescence staining was performed as previously described.<sup>20</sup> MAbs used were as follows: mouse anti-human CXCL12/SDF-1 $\alpha$  (clone 79018, R&D Systems, Minneapolis, MN, USA), CXCR4 (clone 12G5, R&D Systems), and HLA class I (clone W6/32, Thermo Fisher scientific, Waltham, MA, USA). Fluorescein isothiocyanate (FITC)- or Phycoerythrin (PE)-conjugated goat anti-mouse IgG (Biolegend, San Diego, CA, USA) were used as secondary Ab for tracing the primary mAb. For multiple-color phenotyping,  $5 \times 10^5$  cells were directly incubated with FITC-conjugated mouse anti-human CD44 (clone G44-26, BD Pharmingen, Franklin Lakes, NJ, USA), PE-conjugated mouse anti-human HLA-class I (clone W6/32, Abcam, Cambridge, UK), and allophycocyanin (APC)-conjugated mouse anti-human CD24 (clone ML5, Biolegend) mAbs according to the manufacturer's instructions. Labeled cells were then washed three times by PBS plus 2% FBS for following fixation with 1% paraformaldehyde. The fixed samples were analyzed using FACSCalibur (Becton Dickinson, Heidelberg, Germany) and FlowJo software (Tree Star, Ashland, OR, USA).

### Immunofluorescence Confocal Microscopy on Histological Sections

The original LN metastatic lesion of UP-LN1 cell line was fixed in formalin and then embedded in paraffin. Thick tissue sections (5  $\mu$ m) were prepared for subsequent incubation with mAbs as described previously.<sup>23</sup> Blocking was performed with PBS containing 5% BSA for 1 h. The slides were first labeled with FITC-conjugated CD44 antibody (clone G44-26, BD Pharmingen) in 1:10 dilution and then with APC-conjugated CD24 antibody (clone ML5, Biolegend) in 1:5 dilution for overnight at 4<sup>o</sup> C. Hoechst for nucleus stain was performed in 1:500 dilution at room temperature for 15 min. Slides were mounted with a 1:2 solution of glycerol-PBS, sealed by nail oil, and were then imaged by a LSM 510 Meta confocal microscope (Carl Zeiss, Oberkochen, Germany).

### Anchorage-independent Clonogenic Assay

For clonogenic ability of each cell type in either RPMI-1640 medium or in HEScGRO medium, cells were suspended in 0.5% agarose (UltraPure L.M.P. agarose, Invitrogen, Carlsbad, CA, USA) with each medium and then seeded onto the top of 1% agarose with the corresponding medium pre-coated in six-well plates (Corning, Corning, NY, USA). A total volume of 1 ml of the corresponding medium was then added on the top of agarose layer with cells inside. After 20 days (for RPMI medium) or 26 days (for HEScGRO medium) of culture, the plates were stained by crystal violet for quantification of the colonies. The mean colony size was determined by measuring the area of each colony shown in the photos of each wells by the ImageJ software (National Institute of Mental Health, Bethesda, MD, USA).

### Xenotransplantation in NOD/SCID Mice

Xenotransplantation assays of P, A, and F cells were independently carried out in 6- to 8-week-old female NOD/SCID mice purchased from the National Taiwan University Hospital Animal Central Facility, Taipei, Taiwan. P, A, and F cells were separately harvested, washed, and then re-suspended in PBS to make five concentrations from  $10^7$  to  $10^3$  cells/ml by a 10-fold limiting dilution. A volume of 100  $\mu$ l containing each cell dose was injected subcutaneously at the site above the hind leg of each mouse. Tumor growth was monitored every 2–3 days for at least 80 days. The volume of palpable tumor nodules was calculated by the formula,  $\text{mm}^3 = 0.4 \times a \times b^2$ , where  $a$  is the major tumor diameter and  $b$  is the minor diameter perpendicular to the major one.<sup>20</sup>

### RNA Extraction and RT-PCR

Total RNA was extracted separately from P, A, and F cells using TRIzol reagent (Invitrogen), and was reverse transcribed by the use of a First-Strand cDNA Synthesis Kit (Fermentas, Burlington, Canada) according to the manufacturer's instruction. The sense and antisense primer sequences used for the measurement of gene expression level are listed in Supplementary Table S1. The RT-PCR was carried out in a 50  $\mu$ l reaction mixture that containing a final concentration of 50 mM Tris-HCl, (pH 8.3), 50 mM KCl, 1.5 mM  $\text{MnCl}_2$ , 0.2 mM dNTP, 2U of Taq DNA polymerase, 1  $\mu$ l of cDNA as template and 50 pmol of primers. After initial denaturation for 2 min at 95°C, 26 cycles of amplification (at 95°C for 1 min, 60°C for 1 min, and 72°C for 1.5 min) were performed, followed by a 7 min extension at 72°C.

### <sup>51</sup>Chromium-release Cytotoxicity Assay

Two types of effector lymphocytes, LAK and activated CD56<sup>dim</sup>/CD16<sup>+</sup> NK cells, were prepared. Peripheral blood mononuclear cells (PBMCs) were first isolated from healthy donors by density gradient centrifugation with Ficoll-Paque (GE Healthcare Bio-Sciences AB, Uppsala, Sweden) as the sources of effector LAK and cytotoxic CD56<sup>dim</sup>/CD16<sup>+</sup> NK

cell preparations. For LAK preparation, freshly isolated PBMCs were activated by 1000 U/ml recombinant human IL-2 (R&D Systems) in RPMI complete medium for 72 h. CD56<sup>dim</sup>/CD16<sup>+</sup> NK cells were directly separated from PBMCs using a CD56<sup>+</sup>/CD16<sup>+</sup> NK cell isolation kit (Miltenyi Biotec GmbH, Bergisch Gladbach, Germany) according to the manufacturer's instructions. Isolated CD56<sup>dim</sup>/CD16<sup>+</sup> NK cells with purity greater than 99% were further activated by 100 U/ml recombinant human IL-2 in RPMI complete medium for 72 h and then served as another source of effector killer cells to be used in <sup>51</sup>Chromium (<sup>51</sup>Cr)-release cytotoxicity assays. The assay was performed as previously described and the cytotoxicity of effector cells to each cell type was analyzed by % specific lysis at different effector/target ratios.<sup>24</sup> Lytic unit (LU) was calculated for inter-experimental comparison.

### In Vitro Cell Migration and Invasion Assays

P, A, and F cells treated with 1, 10, and 100 U/ml IFN- $\gamma$  (R&D Systems) or without IFN- $\gamma$  were tested by the QCM Chemotaxis Cell Migration and QCM Chemotaxis Cell Invasion Assays, according to the manufacturer's instructions (Millipore Corporation, Billerica, MA, USA). For a cell invasion assay, membrane of each upper chamber was previously coated by ECMatrix, a reconstituted basement membrane matrix of proteins derived from the Engelbreth Holm–Swarm mouse tumor,<sup>25</sup> to mimic *in vivo* basement membrane. The membrane used in cell migration assays was not coated with any material. For both the assays, cells were harvested and re-suspended in RPMI-1640 medium containing 1% FBS. Suspended cells ( $5 \times 10^4$ ) were seeded into the upper chamber. After 24 h at 37°C, cells that had migrated through the membrane to the lower chamber containing 100 ng/ml CXCL12 were collected and lysed. The released cellular nucleic acids were labeled by CyQuant GR dye for quantification.

## RESULTS

### Immunophenotypic Characterization of A and F Subsets in the UP-LN1 Cell Line

We first enriched A and F cells independently from P cells by 10 respective cycles of the enrichment protocols. A cells showed mostly an adherent phenotype in monolayer culture, with only small numbers of floating cells, and could be maintained for the subsequent passages (Figure 1a). On the other hand, F cells showed mostly the floating phenotype with few adherent cells in the subsequent passages (Figure 1a). As compared with the constant adherent morphology of A cell population, F cell population showed a greater tendency to regenerate both floating and adherent cells like the parental cells *in vitro* after several subcultures.

In contrast to the CD44<sup>low</sup>/CD24<sup>high</sup> phenotype of A cells, F cells clearly expressed the opposite phenotype, that is, CD44<sup>high</sup>/CD24<sup>low</sup> (Figure 1b). Upon careful examination of the original LN tumor biopsy sections by immuno-

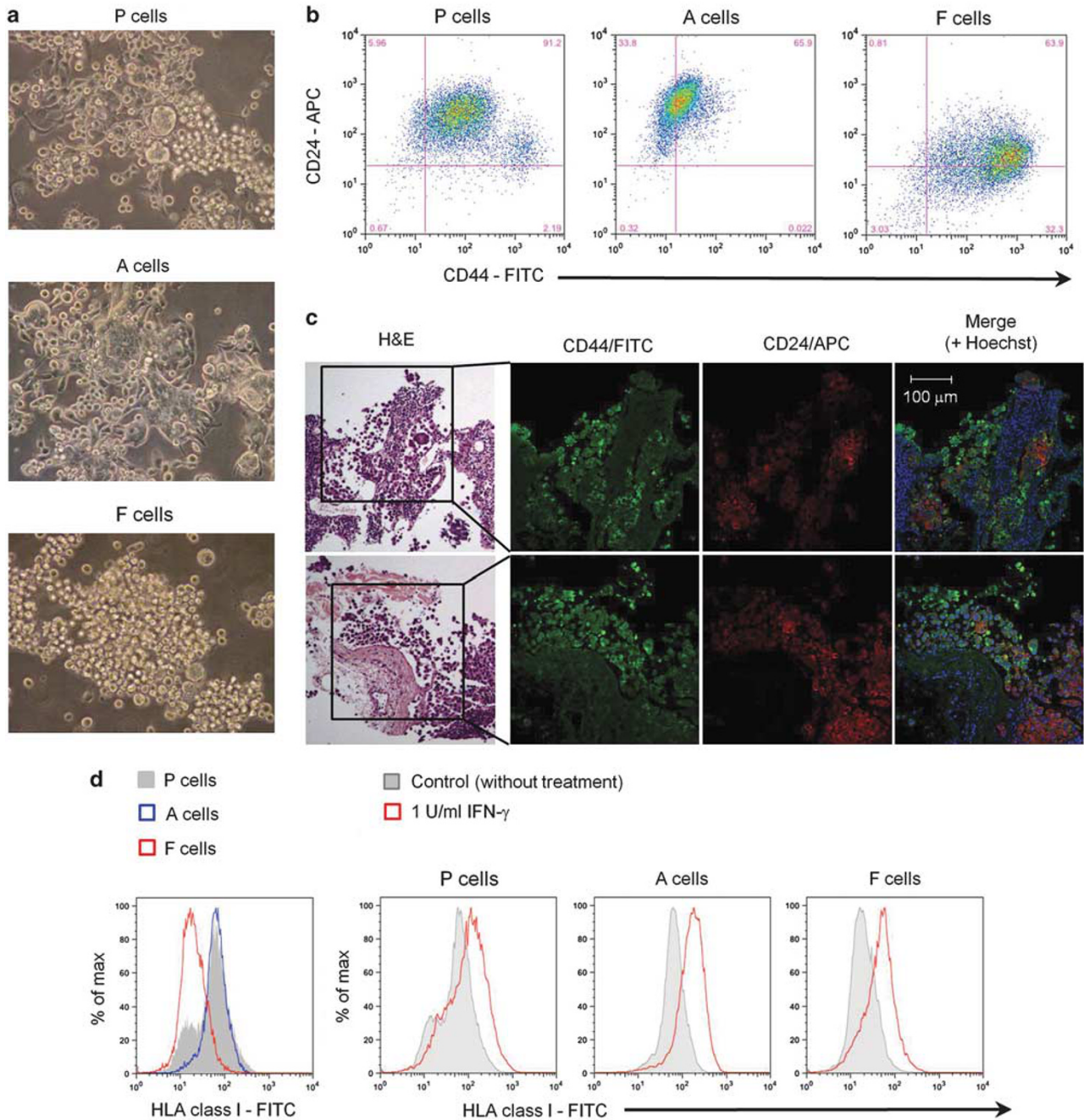


**Figure 1** Morphological and phenotypical features of A and F sub-populations, and the parental UP-LN1 cell line. Representative P, A, and F live cells in culture were shown (a). The expression of CD44/CD24 expression profile of cultured P, A, and F cells were determined by cytofluorometric analysis (b). The CD44<sup>high</sup>/CD24<sup>low</sup> phenotype could also be found in the region with loose tumor cell structure in the original biopsy sections by immunofluorescence confocal microscopy (c). The expression of HLA class I in P, A, and F cells with or without IFN- $\gamma$  treatment for 48 h were assayed by cytofluorometric analysis (d).

fluorescence confocal microscopy, the CD44<sup>high</sup>/CD24<sup>low</sup> phenotype for F cells could be found mainly in the region of loosely associated tumor cells, whereas the CD44<sup>low</sup>/CD24<sup>high</sup> phenotype for A cells could be detected in the region with more compact neoplastic cell areas on the same tumor section (Figure 1c).

F cells showed a greater extent of reduced HLA class I expression than A cells in terms of % positive cells and mean fluorescence intensity (MFI) (Figure 1d). The depressed HLA class I expression in P, A, and F cells could, however, be restored following IFN- $\gamma$  treatment in a dose-dependent manner with different sensitivity (Figure 1d).

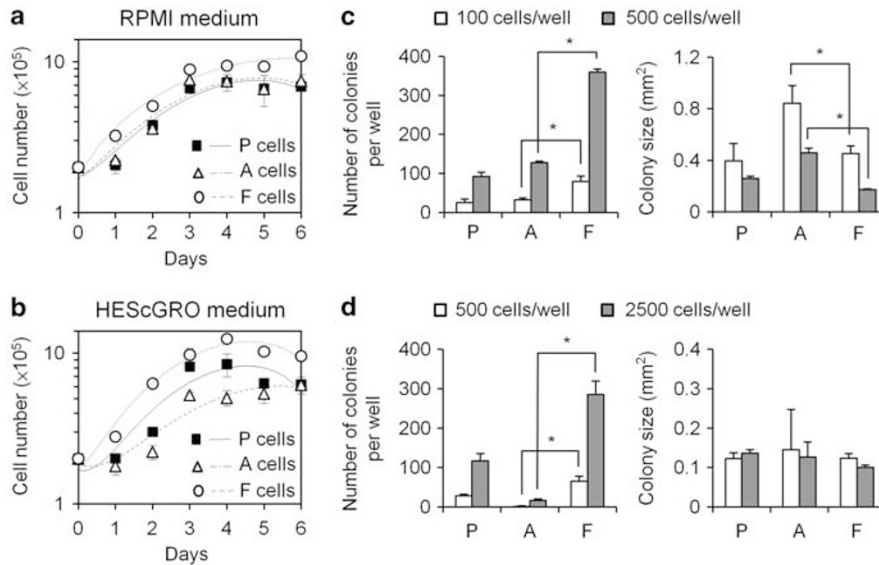


**Figure 2** *In vitro* growth curves and anchorage-independent colony-forming ability of P, A, and F cells. Growth curves of P, A, and F cells cultured as monolayers in RPMI medium (RPMI-1640 + 10% FBS) (a) and HEScGRO medium (b) were determined by counting viable and non-viable cells daily for 6 days. Anchorage-independent clonogenic assays were performed in RPMI medium (c) and HEScGRO medium (d) with mean number of colonies and average colony size indicated. Results are expressed as mean  $\pm$  s.d. ( $n = 3$ ).

### F Cells Exhibited Much Stronger Stem Cell-Like Properties than A Cells *In Vitro*

By the use of DNA microarray, of the 22 575 genes tested, we identified 18 upregulated genes (ratio > two-fold) and 37 downregulated genes in F cells, as compared with A cells.<sup>26</sup> Notably, we found three stem cell-associated genes *PSCA* (prostate stem cell antigen), *ALDH1A1* (aldehyde dehydrogenase), and *CD44* were upregulated to a greater extent in F cells. Further, *ABCA7*, a member of ABC transporter family, was also identified to be upregulated in F cells. These findings suggest that F cells functionally resemble much CSCs.

Growth curves resulting from P, A, and F cells grown in RPMI medium (RPMI-1640 plus 10% FBS) (Figure 2a), and chemically defined HEScGRO medium (Figure 2b) were constructed. F cells were able to grow in both RPMI medium and HEScGRO medium much better than A cells, in terms of population-doubling time and saturation density. In RPMI medium, the population-doubling times for P, A, and F cells were 33.9, 33.9, and 29.8 h; and the saturation densities for P, A, and F cells were  $10.3 \times 10^4$ ,  $10.7 \times 10^4$ , and  $15.4 \times 10^4$  cells/cm<sup>2</sup>, respectively. In HEScGRO medium, the population-doubling times for P, A, and F cells were 30.6, 48.0 and 24.0 h; and the saturation densities were  $12.0 \times 10^4$ ,  $8.8 \times 10^4$ , and  $17.7 \times 10^4$  cells/cm<sup>2</sup>, respectively. Collectively, F cells grew at a faster rate and gave a higher saturation density when cultured in HEScGRO medium than in RPMI medium, whereas the growth of A cells was greatly inhibited in HEScGRO medium. These results may reflect a more stemness nature of F cells as opposed to A cells.

With regard to anchorage-independent clonogenicity in agarose assays, when grown in RPMI medium, greater numbers of colonies were seen in the culture of F cells than in

that of A cells, while generally smaller-sized colonies developed by F cells were evident (Figure 2c, Supplementary Figure S1A). At least two types of colonies (large and small) were developed by P cells. These results suggest that F cells relative to A cells harbored a greater number of self-renewing cells or CSCs. On the other hand, A cells, rather than F cells, contained groups of cells, which could be the fate-committed progenitors with greater ability to proliferate/differentiate, and thus form larger-sized colonies in RPMI medium. In HEScGRO medium, although F cells showed a much higher efficiency in generating colonies than A cells, the average size of colonies generated by F and A cells were similar (Figure 2d). These results revealed that HEScGRO medium, specifically designed for supporting the growth and maintenance of embryonic stem cells, could be used to select cells with stem cell growth features from both F and A cells. The representative images for colonies generated by P, A, and F cells in RPMI medium and HEScGRO medium were depicted in Supplementary Figures S1B and S1C. Our results also imply the qualitative and quantitative differences between A and F cells, with the latter displaying greater stem-like properties.

### F Cells Showed Greater Tumorigenicity than A Cells in NOD/SCID Mice

Relative to A cells, F cells were found to be more tumorigenic and enriched in CSCs (Figure 3a and Table 1). Specifically, F cells could produce tumors with cells injected as low as  $10^3$  cells/mouse with an incidence of 1/9 mice, whereas A cells could produce tumors with at least  $10^5$  cells/mouse injected (8/9 mice). When  $10^5$  cells/mouse were injected into NOD/SCID mice, the mean volume of tumors produced by F cells

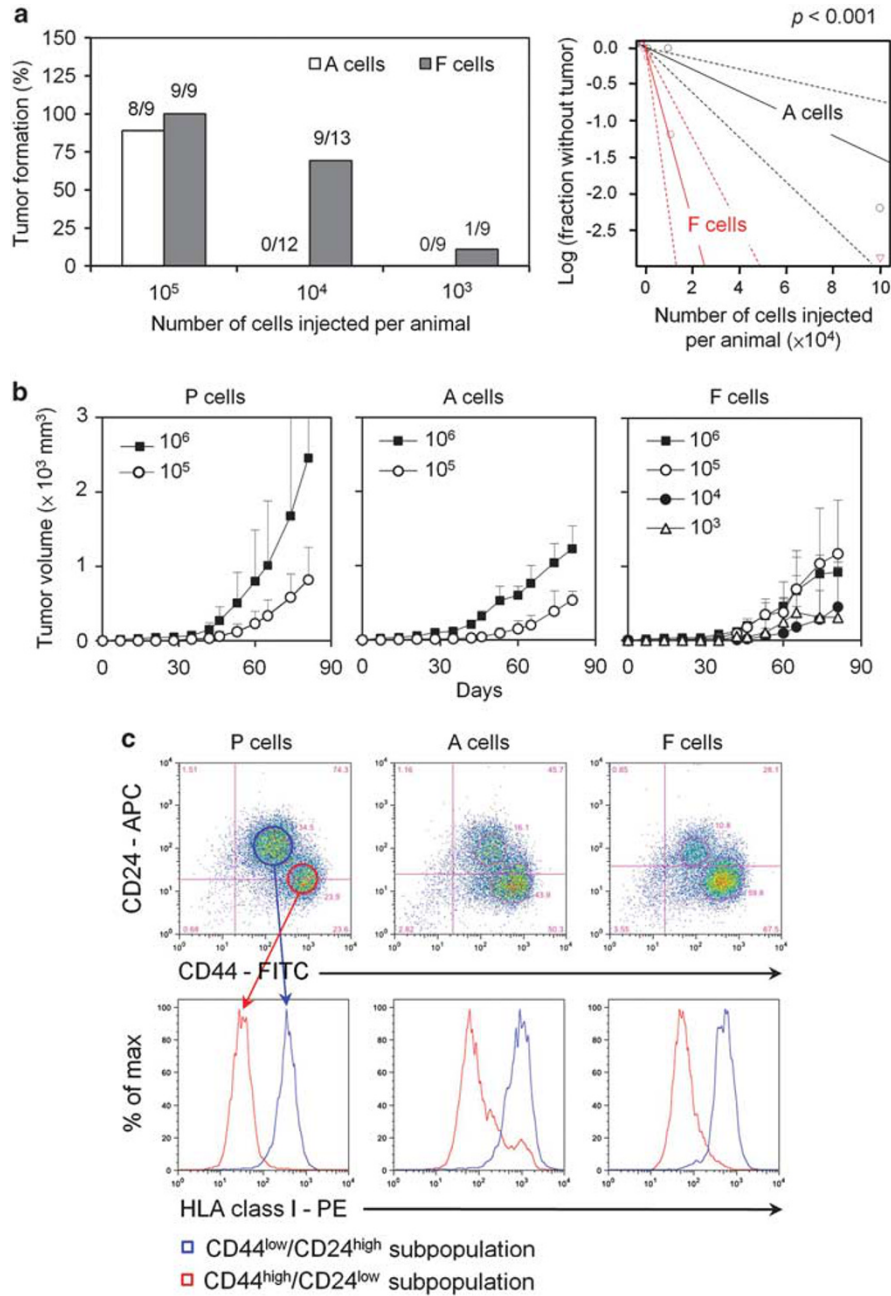


**Figure 3** *In vivo* tumorigenicity of P, A, and F cells in NOD/SCID mice and phenotyping of cultured cells grown from the xenografts. The tumor-infiltrating frequencies of P, A, and F cells were obtained following subcutaneous injection with  $10^5$ ,  $10^4$ , and  $10^3$  cells/mouse (a, left). The extreme limiting dilution analysis based of Poisson distribution was performed using ELDA web tool for estimation of the TIC frequencies of P, A and F cells (a, right). Tumor growth curves of P, A, and F cells obtained from the xenotransplantation experiments are also illustrated (b). Triple-color cytofluorometric analysis was performed to determine the expression of CD44, CD24, and HLA class I in cultured cells from tumors resulting from subcutaneously injection with P, A, and F cells (c).

was similar to that resulting from injecting  $10^6$  F cells/mouse (Figure 3b). Nevertheless, tumors resulting from injection with  $10^5$  A cells were considerably smaller than those injected with  $10^6$  A cells/mouse (Figure 3b). When  $10^6$  cells were injected, P cells generated much larger-sized tumors than either F or A cells (Figure 3b). When  $10^5$  cells were injected, the advantage of P cells for tumor growth was diminished (Figure 3b).

When xenografted tumors produced by A and F cells were processed to re-grow them in culture, both adherent and floating cells appeared in the cell cultures of A as well as F cells, as did the parental UP-LN1 cell line. By flow cytometric analysis, the two CD44<sup>low</sup>/CD24<sup>high</sup> and CD44<sup>high</sup>/CD24<sup>low</sup> phenotypes were again observed in cultured cells from the xenografts resulting from injection with A and F cells (Figure 3c). Moreover, the moderate and low levels of

**Table 1 Tumor-initiating cell frequencies of A and F sub-populations of the UP-LN1 cell line in NOD/SCID mice**

Cell type	Cell number injected <sup>a</sup>					TIC frequency <sup>b</sup> (95% confidence interval)
	10 <sup>6</sup>	10 <sup>5</sup>	10 <sup>4</sup>	10 <sup>3</sup>	10 <sup>2</sup>	
P	9/9 <sup>c</sup>	10/10	0/10	0/10	0/10	1/43 412 (1/86 114–1/21 885)
A	9/9	8/9	0/12	0/8	0/9	1/66 535 (1/135 324–1/32 713)
F	9/9	9/9	9/13	1/9	0/8	1/8573 (1/16 420–1/4476)

<sup>a</sup>Animals were subcutaneously injected with indicated cell numbers.

<sup>b</sup>The tumor-initiating cell (TIC) frequency was estimated by Poisson distribution with the use of the L-Calc limiting dilution analysis software version 1.1 (StemCell technologies) and ELDA web tool (<http://bioinf.wehi.edu.au/software/elda/>).

<sup>c</sup>The number of tumor detected/number of injections.

**Table 2 Differential expression of a panel drug resistance genes in P, A, and F cells of the UP-LN1 cell line determined by RT-PCR**

Gene	Protein	Cell type		
		P	A	F
ABCA2	ABCA2	+ <sup>a</sup>	+	+
ABCA3		+++++	++++	+++++
ABCB1	PGP/MDR1	+	+	++
ABCB5		+++	+	++++
ABCC1	MRP1	+	+	++
ABCC2	MRP2	+	+	+
ABCC3	MRP3	+	+	++++
ABCC4	MRP4	+	+	+
ABCC5	MRP5	+++++	+++	++++
ABCC6	MRP6	+++++	+++++	+++++
ABCC11	MRP8	+++++	+++++	+++++
ABCG2	MXR/BCRP1	++++	+++	++++

Abbreviations: ABC, ATP-bonding cassette; BCRP, breast cancer resistance protein; MDR, multidrug resistance; MRP, multidrug-resistance-associated protein; MXR, mitoxantrone-resistance protein.

<sup>a</sup>% normalized with GAPDH expression (+, <25%; ++, 25–50%; +++, 51–75%; +++++, 76–100%; ++++++, >100%).

surface HLA class I expression were again noted in CD44<sup>low</sup>/CD24<sup>high</sup> and CD44<sup>high</sup>/CD24<sup>low</sup> subsets, respectively (Figure 3c). These results together with *in vitro* results suggest that different classes of CSCs/TICs could be individually harbored in A and F cells.

### **In Vitro F Cells Exhibited Greater Resistances to Multiple Drugs and Non-MHC-restricted Effector Killing Relative to A Cells**

By the semi-quantitative RT-PCR method, some of the multiple drug-resistant (MDR) genes associated with CSCs,

including *ABCG2*,<sup>27</sup> *ABCB5*,<sup>28</sup> *ABCB1*,<sup>29</sup> and *ABCC1*,<sup>30</sup> were identified to be upregulated in F cells as compared with A cells (Table 2). Also, the expression of some other MDR genes such as *ABCA7*, *ABCC3*, and *ABCC5* were elevated in F as compared with A cells. Four remaining genes of the panel were found to be expressed by both F and A cells almost equally. These results suggest that with enriched CSCs, F cells could possibly exhibit greater resistance to multiple drugs as compared with A cells.

Our cytotoxicity results revealed the significant differences in relative susceptibilities of P, A, and F cells to killing by allogeneic LAK cells (Figure 4a) and IL-2-activated CD56<sup>dim</sup>/CD16<sup>+</sup> cytotoxic NK cells (Figure 4b). A cells were extremely sensitive to NK- as well as to LAK-mediated killings at all six effector to target cell ratios tested in three independent experiments. When assessed by lytic units (LUs), the differences between A and F cells in sensitivity to NK- or LAK-mediated cytolysis were both significant ( $P < 0.01$ ) (Supplementary Table S2). These results are in line with the notion that F cells are functionally much closer to CSCs in extreme resistance to non-MHC restricted effector lymphocytes, as compared with A cells.

### **Induction of mCSC in F Cells, but not A Cells, Through IFN- $\gamma$ -mediated Modulation on the CXCR4/CXCL12 Axis**

We next investigated whether any soluble mediators released by activated NK/LAK cells would modulate the metastatic potential of NK/LAK-resistant F cells. Cytofluorometric analysis was carried out to monitor the immunophenotypical changes in A and F cells with or without exposure to the conditioned medium of LAK cell culture. A unique modulation on the CXCR4/CXCL12 axis was found only in F, but not A, cells in response to LAK-conditioned medium (Figure 5a and Supplementary Figures S2A and B). When F cells were cultured in LAK-conditioned medium, the percentage of CXCR4<sup>+</sup> F cells was increased (17.5%) from the basal level (8.4%), whereas the MFI detected in CXCR4<sup>+</sup> cells remained essentially unchanged. Representative histograms of one such cytofluorometric analysis are shown in Figure 5a, in which the peaks of CXCR4<sup>+</sup> expression in terms of MFI were

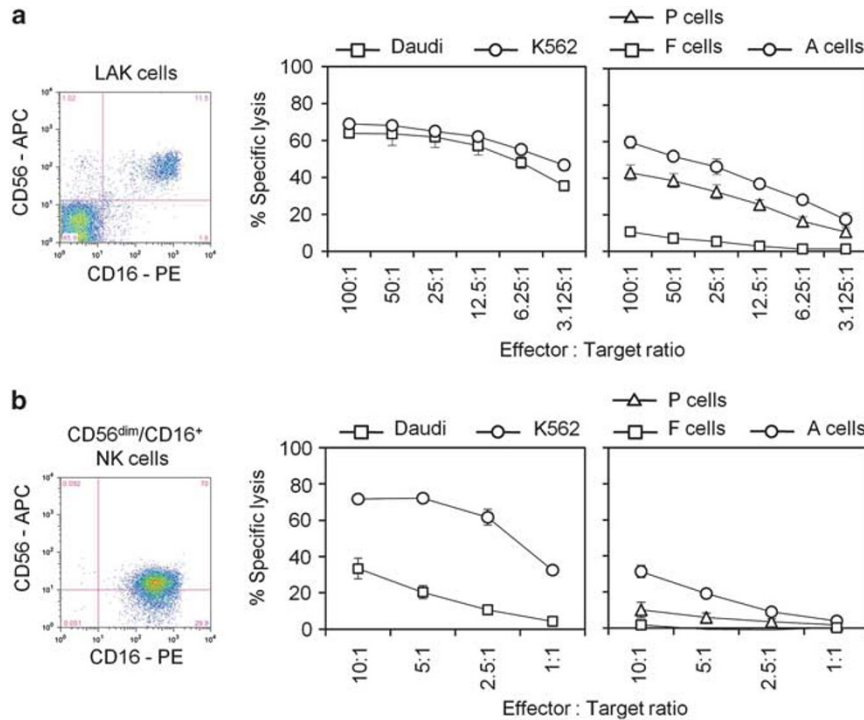


**Figure 4** Susceptibility of P, A, and F cells to non-MHC-restricted effectors. Relative susceptibilities of P, A, and F cells to LAK cells (a) and CD56<sup>dim</sup>/CD16<sup>+</sup> cytotoxic NK cells (b) were determined by 4h-<sup>51</sup>Cr release cytotoxicity assays. The CD56/CD16 immunophenotype of LAK (a, left) and CD56<sup>dim</sup>/CD16<sup>+</sup> cytotoxic NK cells (b, left) were determined by cytofluorometric analysis. Results are expressed as mean ± s.d. (n = 3). The Daudi and K562 cell lines were used as reference targets of NK- and LAK-mediated cytotoxicities because of their differential susceptibilities.

noted to be at the same position in F cells, regardless of whether LAK-conditioned medium was added or not, suggesting that the original CXCR4<sup>+</sup> cells and the induced CXCR4<sup>+</sup> cells expressed a relatively same level or density of the receptor CXCR4 on per cell basis. On the other hand, the percentage of cytoplasmic CXCL12<sup>+</sup> cells was downregulated by 22.3% when F cells were cultured in LAK culture conditioned medium from 94.7% positive cells at the baseline level.

Following IFN- $\gamma$  (1–100 U/ml) treatment, the dose-dependent changes on CXCR4/CXCL12 expression profiles of P, A, and F cells turned out to be very similar to those obtained with the respective cells in the presence of LAK culture conditioned medium (Figure 5b). Specifically, the IFN- $\gamma$ -mediated induction of positive and totally negative sub-populations for surface CXCR4 and cytoplasmic CXCL12 expression in F cells, but not in A cells, was in an all-or-none manner. We also provide bar-type illustrations to more clearly show the qualitative analysis of the same data (Supplementary Figures S2C and D).

For cell migration, A cells showed a delayed response when the dose of IFN- $\gamma$  was higher than 10 U/ml, whereas F cells started to respond to IFN- $\gamma$  with a dose as low as 1 U/ml (Figure 5c). For cell invasiveness, F cells started showing the response to IFN- $\gamma$  at 10 U/ml, but the response of A cells to IFN- $\gamma$  could only be observed when 100 U/ml IFN- $\gamma$  was used (Figure 5d). Overall, these observations demonstrated that the CXCR4<sup>+</sup> mCSCs with elevated metastatic potential

could be specifically induced only from the NK/LAK-resistant F cell subset by IFN- $\gamma$ .

## DISCUSSION

In this study, we characterized the CSC heterogeneity in the CEA-producing UP-LN1 carcinoma cell line with the intent to better understand the role of CSCs in this malignancy. The F and A cell subsets can now be distinguished on the basis of their distinct immunophenotypes, namely, CD44<sup>high</sup>/CD24<sup>low</sup> for F cells and CD44<sup>low</sup>/CD24<sup>high</sup> for A cells, which could also be correlated with loosely distributed single or small clumps of tumor cells and compact tumor cells, respectively, in the patient's LN tumor tissue.

Our results from the experiments of *in vivo* xenotransplantation and *in vitro* anchorage-independent colony formation suggest that F and A cells may have provided different niches to harbor at least two different classes of CSCs. The interactions among the CSCs and differentiated non-CSCs within a tumor have rarely been addressed. For example, upon chemotherapy, the CXCR1<sup>+</sup> breast CSCs can overcome FasL-induced apoptosis by receiving the IL-8 signal released from CXCR1<sup>-</sup> non-CSCs.<sup>31</sup> In our xenotransplantation study, we noted that some cooperation between A and F cells might have existed in order for P cells to develop larger-sized tumors when compared with A or F cells alone. Such cooperation for optimal tumor growth appeared to be dictated by the critical numbers and the ratio of



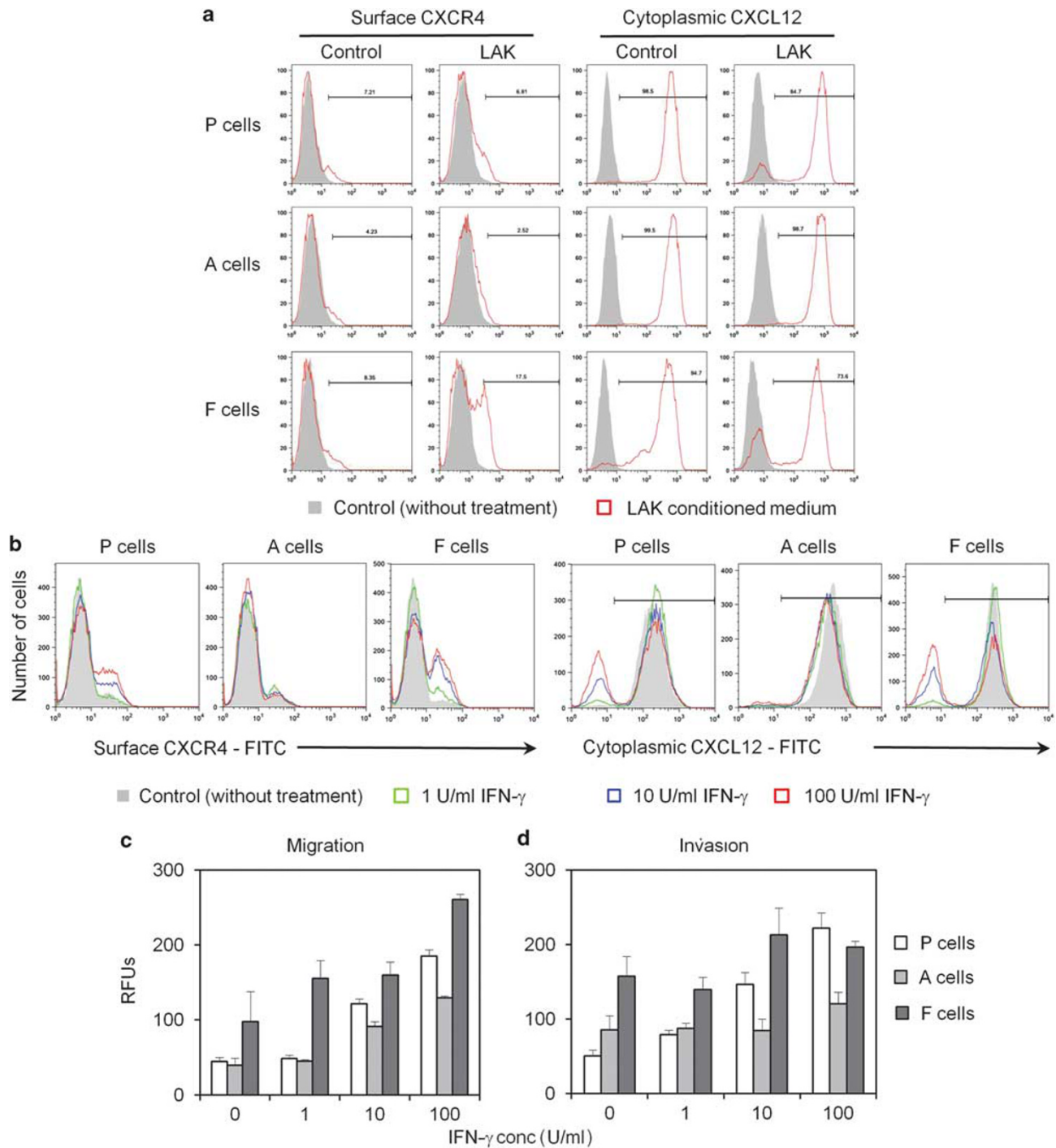


**Figure 5** IFN- $\gamma$  mediated-induction of mCSCs through acquisition of CXCR4 surface expression on the CXCR4/CXCL12 axis in F cells. Cells treated with LAK culture conditioned medium (a) and different concentrations of IFN- $\gamma$  (b) for 48 h were harvested and subjected to immunophenotyping for the expression of surface CXCR4 and cytoplasmic CXCL12. The QCM fluorimetric cell migration and invasion assays were used for quantification of cell migration (c) and invasion (d) toward CXCL12 chemoattraction, respectively. Results are expressed as mean  $\pm$  s.d. ( $n = 3$ ).

A and F cells in the parental tumor cells. It is likely that some type of cooperation for aggressive tumor growth between the different subset of CSCs in F and A cells may also exist. Interestingly, similar modulation affecting the degrees of tuomrigenicity *via* the interactions between clonal variants

harboring different classes of CSCs and non-CSC tumor cells of a squamous cell carcinoma cell line has also been reported recently,<sup>32</sup> although other factors such as angiogenic activity and stromal interaction could also be involved in the co-operation process.

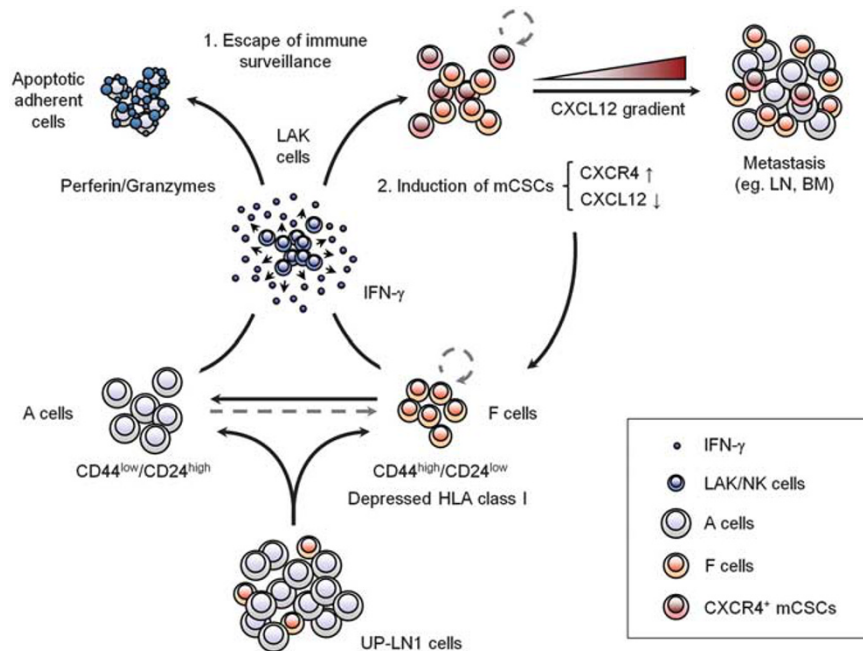


**Figure 6** Proposed mechanism of induction of mCSCs for UP-LN1 cells to metastasize. To make UP-LN1 cells to metastasize, the floating cells serve as a major reservoir for CSCs with extreme resistance to LAK-mediated killing and concomitantly with high susceptibility to IFN- $\gamma$ -mediated induction of metastatic potential via generation of mCSCs. Then, the induction of CXCR4<sup>+</sup> mCSCs with reduced release of CXCL12 at the same time by the tumor cells could create a favorable microenvironment for CXCR4-bearing mCSCs to migrate toward a site where a greater CXCL12 gradient is present, such as LN, bone marrow, or other distant organ.

Operationally, the different classes of CSCs have been believed to come from either clonal evolution of a given cancer through successive selective pressures and/or cancer progression through clonal coexistence or sequential clonal existence.<sup>33</sup> During cancer progression, the emergence of new classes of CSCs could have occurred as a result of nutritional or immunological pressures, or could have been induced by therapy. If these different classes of CSCs in F and A cells do exist, additional work is needed to determine what the exact differences are. Although the biological significance of the coexistence of A and F cells in the UP-LN1 cell line/tumor remains elusive, it appears that using A cells as a bait to be killed by activated NK/LAK cells, the tumor is, in turn, to fool the host immune system by utilizing IFN- $\gamma$  released from these immune effector cells to induce the CXCR4<sup>+</sup> mCSCs in F cells to a greater number, thereby leading to the LN and/or distant metastatic site migration of CXCR4<sup>+</sup> mCSCs (Figure 6). Thus, F cells appear to be destined to have a greater role in tumor survival, tumorigenicity, perpetuation, and dissemination in the tumor-bearing host.

By the expression of surface CXCR4, tumor cells acquire the properties qualifying them to sense chemoattractants, invade tissue barriers, and migrate to a secondary organ to form a metastasis.<sup>34,35</sup> Furthermore, the CXCR4<sup>+</sup> subpopulation within the CD133<sup>+</sup> CSCs has been reported to be the mCSCs with increased metastatic potential in pancreatic cancer.<sup>36</sup> Following this finding, one emerging question is 'How could the CXCR4 and CXCL12 expression be regulated

in mCSCs and tumor metastasis?' Dalerba and Clarke<sup>37</sup> proposed three possible models with either a reversible or a non-reversible manner in an attempt to explain how the CXCR4 was being expressed by CSCs, followed by metastasis. In light of our current findings, we favor the notion that the CXCR4<sup>+</sup> mCSCs originated from CXCR4<sup>-</sup> CSCs through specific signals such as, IFN- $\gamma$ ,<sup>38,39</sup> other cytokines, HGF,<sup>40</sup> and/or hypoxia in a reversible manner.<sup>41</sup>

IFN- $\gamma$  could induce the expression of CXCR4 with concomitant diminishment of CXCL12 production in F cells to create a microenvironment with low level CXCL12. Subsequently, such microenvironment may lead the induced CXCR4<sup>+</sup> mCSCs within F cells to sense the CXCL12 gradient much easier and then be attracted to a so-called 'pre-metastatic niche', such as LN and bone marrow, which are known to be with abundant CXCL12 secretion. The 'pre-metastatic niche' has sufficient numbers of stromal fibroblastic cells and/or bone marrow-derived mesenchymal stem cells, which are rich in secretion of CXCL12.<sup>42</sup> It will be therefore important to determine whether CXCL12, found abundantly in the cytoplasm of A cells, in the presence or absence of IFN- $\gamma$  or LAK culture conditioned medium, are indeed being proportionally secreted into the culture medium.

Although F cells, rather than A cells, were shown to be modulated on the CXCR4/CXCL12 axis, migration and invasiveness toward the CXCL12 gradient were upregulated in both A and F cells with different degrees of sensitivity following IFN- $\gamma$  treatment. The moderate enhancement in

migration and invasion of A cells may be partially due to the modulation on another receptor of CXCL12 on the same tumor cell surface, namely CXCR7.<sup>43</sup> The effect of IFN- $\gamma$  on cell mobility may also directly contribute to the upregulation of migration and invasiveness. Further experiments are needed to evaluate the effect of IFN- $\gamma$  in modulation on tumor metastasis by injection of F and A cells with and without IFN- $\gamma$  treatment *via* either a footpad or an intravenous route into immunodeficient mice.

The ability of tumors to escape from the host immunosurveillance could also be due to the presence of CSCs.<sup>44,45</sup> It has been reported that in breast cancer, the CD44<sup>high</sup>/CD24<sup>low</sup>/Her2<sup>low</sup> CSCs with elevated clonogenicity, tumorigenicity, and self-renewal ability could be selected out from a bulk tumor population by NK cells through trastuzumab-induced antibody dependent cell-mediated cytotoxicity.<sup>46</sup> Moreover, it has been shown that ABCB5<sup>+</sup> malignant melanoma TICs not only expressed lower levels of surface HLA class I molecules as compared with their ABCB5<sup>-</sup> counterpart, but also acquired the ability to inhibit IL-2-dependent activation of effector T cells by the induction of CD4<sup>+</sup>/CD25<sup>+</sup>/Foxp3<sup>+</sup> regulatory T cells.<sup>47</sup> Our study shows that the CD44<sup>high</sup>/CD24<sup>low</sup> F cells harboring the majority of the CSCs of UP-LN1 cells exhibit the extreme resistance to NK/LAK-mediated cytotoxicity. Furthermore, the expression of surface HLA class I was observed to be tightly regulated following the transformation between F and A cells. Thus, we believe that three events, the impaired expression of surface HLA class I, extreme resistance to NK/LAK-mediated cytotoxicity, and more enhanced expression of many CSC-associated genes/markers in F cells are not all coincidental. Downregulation of HLA class I seems to be an efficient strategy developed by tumor cells to escape from both CTL and NK cell immunosurveillance, as the expression thresholds of HLA class I required to adequately activate CTL and NK cells may be different.<sup>23,48</sup> As HLA class I molecules are the inhibitory signal for NK cells to avoid killing of normal cells, this fuzzy area between the activation of CTLs and NK cells provides a safe zone for tumor cells with downregulated HLA class I expression to avoid successful presentation of tumor antigen to trigger CTL killing and activation of NK-mediated cytotoxicity of tumor cells. Although the relationship between the defects of HLA class I expression and CSC properties remains unclear at present, the link between depressed HLA class I expression and CSCs may be an important issue to be investigated further.

In summary, we have herein documented the morphological (floating and adherent), immunophenotypic (CD44<sup>high</sup>/CD24<sup>low</sup> and CD44<sup>low</sup>/CD24<sup>high</sup>), and clonogenic heterogeneity of the CSCs within UP-LN1 cells in a functional sense, such as cell-cell cooperation for tumor growth, escape from NK/LAK-mediated killing, and IFN- $\gamma$ -mediated induction of mCSCs. Also, we demonstrated for the first time that activated NK/LAK cells and their secreted IFN- $\gamma$  could function as a promoter rather than a cytotoxic effector to

LAK-resistant CD44<sup>high</sup>/CD24<sup>low</sup> floating tumor cells, which are enriched in CSCs for the generation of CXCR4<sup>+</sup> mCSCs. In order for the tumor to proceed progression, the F cells themselves turned out to be a niche for the predominant CSCs/mCSCs by their unique abilities to initiate tumors in and migrate/invade toward an appropriate tissue micro-environment, in spite of the pressure from the host immunosurveillance. Whether these findings are restricted to the UP-LN1 unique cell line/tumor or not has to await further studies by evaluating floating and adherent cells of additional GI cancers and their cell lines. The observed IFN- $\gamma$ -mediated induction of CXCR4<sup>+</sup> mCSCs from F cells suggests that immunotherapy with non-MHC-restricted effectors such as NK/LAK therapy will not be advised for cancer patients, in whom the expression of CXCR4 on their tumor cells is inducible in the CSC subset by IFN- $\gamma$ . Thus, IFN- $\gamma$  is indeed a double-edged sword, and should be put to therapeutic use very carefully. Besides the non-MHC-restricted effectors CTLs have been reported to be effective in recognition and destruction of brain tumor stem-like initiating cells.<sup>49</sup> Also  $\gamma\delta$ T lymphocytes, another class of non-MHC-restricted effectors, have been shown to exert efficient killing of colon CSCs.<sup>50</sup> Whether  $\gamma\delta$ T cells and MHC-restricted T-cell-based immunotherapy in combination with chemotherapy can be used effectively to eradicate the CXCR4<sup>+</sup> mCSCs and/or their niche, CD44<sup>high</sup>/CD24<sup>low</sup> F cells, remains to be seen. Recently, a high-throughput screening for a variety of inhibitors of CSCs including nutraceuticals has been initiated,<sup>51,52</sup> and this may be an important step toward eradication of CSCs, thus enhancing the strategic options of curing cancer.

Supplementary Information accompanies the paper on the Laboratory Investigation website (<http://www.laboratoryinvestigation.org>)

#### ACKNOWLEDGEMENTS

This study was supported in part by grants from the National Science Council of Taiwan (NSC97-2314-B-182-017; NSC98-2314-B-182-018), the Department of Health of Taiwan (DOH100-TD-C-111-008), and the Chang Gung Medical Research Fund (CMRPD170042). We wish to thank Cherry Tzu-Ru Chang, Shaw-Ching Soong, and Chuan-Tien Hung for skillful technical assistance.

#### DISCLOSURE/CONFLICT OF INTEREST

The authors declare no conflict of interest.

1. Croker AK, Allan AL. Cancer stem cells: implications for the progression and treatment of metastatic disease. *J Cell Mol Med* 2008;12:374–390.
2. Lapidot T, Sirard C, Vormoor J, *et al*. A cell initiating human acute myeloid leukaemia after transplantation into SCID mice. *Nature* 1994;367:645–648.
3. Singh SK, Hawkins C, Clarke ID, *et al*. Identification of human brain tumour initiating cells. *Nature* 2004;432:396–401.
4. Bao S, Wu Q, McLendon RE, *et al*. Glioma stem cells promote radioresistance by preferential activation of the DNA damage response. *Nature* 2006;444:756–760.
5. Al-Hajj M, Wicha MS, Benito-Hernandez A, *et al*. Prospective identification of tumorigenic breast cancer cells. *Proc Natl Acad Sci USA* 2003;100:3983–3988.

6. Li C, Heidt DG, Dalerba P, *et al*. Identification of pancreatic cancer stem cells. *Cancer Res* 2007;67:1030–1037.
7. Wang J, Guo LP, Chen LZ, *et al*. Identification of cancer stem cell-like side population cells in human nasopharyngeal carcinoma cell line. *Cancer Res* 2007;67:3716–3724.
8. Zou GM. Cancer initiating cells or cancer stem cells in the gastrointestinal tract and liver. *J Cell Physiol* 2008;217:598–604.
9. Reya T, Morrison SJ, Clarke MF, *et al*. Stem cells, cancer, and cancer stem cells. *Nature* 2001;414:105–111.
10. Pardal R, Clarke MF, Morrison SJ. Applying the principles of stem-cell biology to cancer. *Nat Rev Cancer* 2003;3:895–902.
11. Bergfeld SA, DeClerck YA. Bone marrow-derived mesenchymal stem cells and the tumor microenvironment. *Cancer Metastasis Rev* 2010;29:249–261.
12. Solinas G, Marchesi F, Garlanda C, *et al*. Inflammation-mediated promotion of invasion and metastasis. *Cancer Metastasis Rev* 2010;29:243–248.
13. Dean M, Fojo T, Bates S. Tumour stem cells and drug resistance. *Nat Rev Cancer* 2005;5:275–284.
14. Rich JN. Cancer stem cells in radiation resistance. *Cancer Res* 2007;67:8980–8984.
15. Kawasaki BT, Farrar WL. Cancer stem cells, CD200 and immunoevasion. *Trends Immunol* 2008;29:464–468.
16. Allan AL, Vantuyghem SA, Tuck AB, *et al*. Tumor dormancy and cancer stem cells: implications for the biology and treatment of breast cancer metastasis. *Breast Dis* 2006;26:87–98.
17. Ji J, Chen X, Leung SY, *et al*. Comprehensive analysis of the gene expression profiles in human gastric cancer cell lines. *Oncogene* 2002;21:6549–6556.
18. Liao SK, Peng YP, Shen YC, *et al*. Chromosomal abnormalities of a new nasopharyngeal carcinoma cell line (NPC-BM1) derived from a bone marrow metastatic lesion. *Cancer Genet Cytogenet* 1998;103:52–58.
19. Mori M, Mimori K, Yoshikawa Y, *et al*. Analysis of the gene-expression profile regarding the progression of human gastric carcinoma. *Surgery* 2002;131:539–547.
20. Chang CTR, Weng WH, Chou AS, *et al*. Immunophenotypic and molecular cytogenetic features of the cell line UP-LN1 established from a lymph node metastasis of a poorly-differentiated carcinoma. *Anticancer Res* 2005;25:683–691.
21. Langlois AJ, Holder Jr WD, Iglehart JD, *et al*. Morphological and biochemical properties of a new human breast cancer cell line. *Cancer Res* 1979;39:2604–2613.
22. Bates RC, Edwards NS, Yates JD. Spheroids and cell survival. *Crit Rev Oncol Hematol* 2000;36:61–74.
23. Hsieh CH, Hsu YJ, Chang CC, *et al*. Total HLA class I loss in a sarcomatoid renal carcinoma cell line caused by the coexistence of distinct mutations in the two encoding  $\beta$ 2-microglobulin genes. *Cancer Immunol Immunother* 2009;58:395–408.
24. Law KS, Chen HC, Liao SK. Non-cytotoxic and sublethal paclitaxel treatment potentiates the sensitivity of cultured ovarian tumor SKOV-3 cells to lysis by lymphokine-activated killer cells. *Anticancer Res* 2007;27:841–850.
25. Terranova VP, Hujanen ES, Loeb DM, *et al*. Use of a reconstituted basement membrane to measure cell invasiveness and select for highly invasive tumor cells. *Proc Natl Acad Sci USA* 1986;83:465–469.
26. Kang CC. Mechanisms involved in the high susceptibility of adherent cells but not floating cells of the UP-LN1 carcinoma cell line to lymphokine-activated killer-mediated cytotoxicity. MSc thesis (Supervisor: Dr S-K Liao) Chang Gung University, Taiwan; 2006.
27. Hirschmann-Jax C, Foster AE, Wulf GG, *et al*. A distinct 'side population' of cells with high drug efflux capacity in human tumor cells. *Proc Natl Acad Sci USA* 2004;101:14228–14233.
28. Schatton T, Murphy GF, Frank NY, *et al*. Identification of cells initiating human melanomas. *Nature* 2008;451:345–349.
29. Keshet GI, Goldstein I, Itzhaki O, *et al*. MDR1 expression identifies human melanoma stem cells. *Biochem Biophys Res Commun* 2008;368:930–936.
30. Zhu Z, Hao X, Yan M, *et al*. Cancer stem/progenitor cells are highly enriched in CD133<sup>+</sup>CD44<sup>+</sup> population in hepatocellular carcinoma. *Int J Cancer* 2010;129:2067–2078.
31. Ginestier C, Liu S, Diebel ME, *et al*. CXCR1 blockade selectively targets human breast cancer stem cells *in vitro* and in xenografts. *J Clin Invest* 2010;120:485–497.
32. Cameron SR, Dahler AL, Endo-Munoz LB, *et al*. Tumor-initiating activity and tumor morphology of HNSCC is modulated by interactions between clonal variants within the tumor. *Lab Invest* 2010;90:1594–1603.
33. Alison MR, Lim SM, Nicholson LJ. Cancer stem cells: problems for therapy? *J Pathol* 2011;223:147–161.
34. Kucia M, Jankowski K, Reza R, *et al*. CXCR4-SDF-1 signalling, locomotion, chemotaxis and adhesion. *J Mol Histol* 2004;35:233–245.
35. Muller A, Homey B, Soto H, *et al*. Involvement of chemokine receptors in breast cancer metastasis. *Nature* 2001;410:50–56.
36. Hermann PC, Huber SL, Herrler T, *et al*. Distinct populations of cancer stem cells determine tumor growth and metastatic activity in human pancreatic cancer. *Cell Stem Cell* 2007;1:313–323.
37. Dalerba P, Clarke MF. Cancer stem cells and tumor metastasis: first steps into uncharted territory. *Cell Stem Cell* 2007;1:241–242.
38. Hosokawa Y, Hosokawa I, Ozaki K, *et al*. CXCL12 and CXCR4 expression by human gingival fibroblasts in periodontal disease. *Clin Exp Immunol* 2005;141:467–474.
39. Katayama A, Ogino T, Bandoh N, *et al*. Expression of CXCR4 and its down-regulation by IFN- $\gamma$  in head and neck squamous cell carcinoma. *Clin Cancer Res* 2005;11:2937–2946.
40. Maroni P, Bendinelli P, Matteucci E, *et al*. HGF induces CXCR4 and CXCL12-mediated tumor invasion through Ets1 and NF- $\kappa$ B. *Carcinogenesis* 2007;28:267–279.
41. Struckmann K, Mertz K, Steu S, *et al*. pVHL co-ordinately regulates CXCR4/CXCL12 and MMP2/MMP9 expression in human clear-cell renal cell carcinoma. *J Pathol* 2008;214:464–471.
42. Psaila B, Kaplan RN, Port ER, *et al*. Priming the 'soil' for breast cancer metastasis: the pre-metastatic niche. *Breast Dis* 2006;26:65–74.
43. Maksym RB, Tarnowski M, Grymala K, *et al*. The role of stromal-derived factor-1—CXCR7 axis in development and cancer. *Eur J Pharmacol* 2009;625:31–40.
44. Chikamatsu K, Takahashi G, Sakakura K, *et al*. Immunoregulatory properties of CD44<sup>+</sup> cancer stem-like cells in squamous cell carcinoma of the head and neck. *Head Neck* 2010.
45. Di Tomaso T, Mazzoleni S, Wang E, *et al*. Immunobiological characterization of cancer stem cells isolated from glioblastoma patients. *Clin Cancer Res* 2010;16:800–813.
46. Reim F, Dombrowski Y, Ritter C, *et al*. Immunoselection of breast and ovarian cancer cells with trastuzumab and natural killer cells: selective escape of CD44<sup>high</sup>/CD24<sup>low</sup>/HER2<sup>low</sup> breast cancer stem cells. *Cancer Res* 2009;69:8058–8066.
47. Schatton T, Schutte U, Frank NY, *et al*. Modulation of T-cell activation by malignant melanoma initiating cells. *Cancer Res* 2010;70:697–708.
48. Chang CC, Ferrone S. NK cell activating ligands on human malignant cells: molecular and functional defects and potential clinical relevance. *Semin Cancer Biol* 2006;16:383–392.
49. Brown CE, Starr R, Martinez C, *et al*. Recognition and killing of brain tumor stem-like initiating cells by CD8<sup>+</sup> cytolytic T cells. *Cancer Res* 2009;69:8886–8893.
50. Todaro M, D'Asaro M, Caccamo N, *et al*. Efficient killing of human colon cancer stem cells by gammadelta T lymphocytes. *J Immunol* 2009;182:7287–7296.
51. Gupta PB, Onder TT, Jiang G, *et al*. Identification of selective inhibitors of cancer stem cells by high-throughput screening. *Cell* 2009;138:645–659.
52. Sarkar FH, Li Y, Wang Z, *et al*. The role of nutraceuticals in the regulation of Wnt and Hedgehog signaling in cancer. *Cancer Metastasis Rev* 2010;29:383–394.